Journal of Hazardous Materials 209–210 (2012) 271–277

Contents lists available at SciVerse ScienceDirect

Journal of Hazardous Materials

journal homepage: www.elsevier.com/locate/jhazmat

Microwave degradation of methyl orange dye in aqueous solution in the presence of nano-TiO_2-supported activated carbon (supported-TiO_2/AC/MW)

Zhaohong Zhang[a,*], Yao Xu[a], Xiping Ma[a], Fangyi Li[a], Danni Liu[a], Zhonglin Chen[a], Fengqiu Zhang[a], Dionysios D. Dionysiou[b,**]

[a] College of Environment, Liaoning University, Shenyang 110036, People's Republic of China
[b] Environmental Engineering and Science Program, University of Cincinnati, Cincinnati, OH 45221-0012, USA

ARTICLE INFO

Article history:
Received 26 September 2011
Received in revised form
17 December 2011
Accepted 5 January 2012
Available online 20 January 2012

Keywords:
Azo dye
Activated carbon
Degradation
Microwave
Supported TiO_2

ABSTRACT

In this study, nano-TiO_2-supported activated carbon (TiO_2/AC) was developed for the microwave (MW) degradation of an azo dye, methyl orange (MO), selected as a model contaminant in aqueous solution. The effects of selected process parameters such as supported TiO_2 content, MW irradiation time, initial MO concentration, catalyst dose, and solution pH on the degradation were assessed in detail. The results showed that the supported TiO_2 on AC could be excited resulting in the production of hydroxyl radical (•OH) in aqueous solution under MW irradiation, which significantly enhanced the performance of AC/MW process for the degradation of MO. Also, the supported-TiO_2/AC displayed higher catalytic activity than AC alone under MW irradiation. By comparison, the supported-TiO_2/AC/MW process exhibited several advantages, including high degradation rate, short irradiation time, no residual intermediates and no secondary pollution. Hence, it shows to be a promising technology for the destruction of organic contaminants in dye treatment applications.

1. Introduction

Azo dyes have been long and widely employed for coloring and printing in many industrial applications [1,2]. Azo dyes with one or several azo bonds (—N=N—) constitute the largest group of dyes and represent more than half of the global dye production [3]. However, in many developing countries, during the extensive production and use of dyes, the concentrated dye wastewater is drained into aquatic systems without being effectively treated [4,5]. These effluents are highly variable in composition with relatively low BOD and high COD contents and also are typically characterized by strong color, recalcitrance, high salinity, high temperature and variable pH [6]. They have a severe impact on water and soil since they are extremely resistant to microbial degradation, and thus can be unavoidably converted to toxic or even carcinogenic compounds [7–9].

Among the reported processes for the treatment of these azo dye contaminated wastes, coagulation–flocculation, membrane processes, and adsorption are unable to completely eliminate the dye pollutants, but merely transfer dyes from one phase to another. Thus, secondary pollution is easily caused [10]. In recent years, several new technologies for oxidation of organic pollutants in water have been reported. Among them, Fenton-like technologies are suitable for the treatment of contaminants at high strength waste, but incomplete degradation usually occurs. Photocatalytic technology that is considered to be a popular remediation technology for the treatment of organic contaminants is only suitable for transparent and low concentration solutions, and it usually needs a significantly long irradiation time before it achieves complete mineralization [11,12]. Also, several other AOPs can yield by-products that are sometimes more poisonous than the dyes themselves [13]. Therefore, it is necessary for scientists and engineers to develop new technologies or improve old processes to treat azo dye-contaminated wastewater before discharge.

Recently, there have been some reports on wastewater treatment using microwave (MW)-assisted degradation technologies [14,15]. Among them, a type of MW-enhanced photocatalytic technology using TiO_2/activated carbon (AC) with an electrodeless discharge lamp (EDL) that could be excited to generate ultraviolet (UV) light under MW irradiation has been reported by He [16] and Liu [17]. The MW-enhanced photocatalytic degradation was conducted in a MW-EDL system for the degradation of Rhodamine B. However, the reaction apparatus was conducted using UV light combined with MW. Also, it took a longer time (more than 30 min), and thus higher consumption of MW energy, before complete photocatalytic degradation was achieved. In addition, another

* Corresponding author. Tel.: +86 24 62205173; fax: +86 24 62204818.
** Co-Corresponding author. Tel.: +1 513 5560724; fax: +1 513 5564162.
E-mail addresses: lnuhjhx@163.com, lnuhjhx@sina.com (Z.H. Zhang), dionysios.d.dionysiou@uc.edu (D.D. Dionysiou).

0304-3894/$ – see front matter © 2012 Elsevier B.V. All rights reserved.
doi:10.1016/j.jhazmat.2012.01.021

type of photocatalytic technology on the degradation of methyl orange by using TiO_2/AC composite as photocatalyst prepared by a hydrothermal method was reported by Wang [18] and Liu [19]. In their studies, the degradation reaction was also conducted in a system equipped with a UV lamp. Results show that the AC helps the adsorption of contaminants on the surface of TiO_2 or TiO_2 composite, in which MW is also used to assist in the photocatalytic degradation.

In our previous work, the degradation kinetics of Congo red or sodium dodecyl benzene sulfonate (SDBS) in aqueous solution using AC/MW was studied [20,21]. For this MW-induced degradation technology, it was considered that under MW irradiation some "hot spots" may be generated on the surface of AC due to its non-uniformity. The organic pollutants could be adsorbed and then degraded by these "hot spots". However, this method had certain limitations when considering the treatment of organics at low concentration, residual pollutants, and reaction by-products. It was difficult for some of these pollutants to approach the "hot spots" in aqueous solution, considering that such "hot spots" are believed to have very short lifetime. Furthermore, we investigated the MW-induced degradation of SDBS in aqueous solution in the presence of AC mixed with TiO_2 or ZnO [22]. The degradation kinetics was better, but there were some problems of separating and recycling TiO_2 or ZnO and AC for reuse. In this current study, an alternative improved method concerning the use of nano-TiO_2 supported on the surface of AC in a MW system (TiO_2/AC/MW) is proposed. It was anticipated that the degradation kinetics as of such materials as well as the possibility for their recycling and reuse would be enhanced. The supported TiO_2 can absorb the heat energy of "hot spots" on the surface of AC under MW irradiation and could be excited to generate electron–hole pairs to form hydroxyl radicals (•OH) in aqueous solution, which can non-selectively attack organic contaminants [23]. Also, the catalytic activities of the supported-TiO_2/AC and AC alone under MW irradiation were compared. The results showed that the supported-TiO_2 significantly enhanced the AC/MW degradation kinetics and the supported-TiO_2/AC displayed better catalytic activity under MW irradiation. By comparison, the supported-TiO_2/AC/MW process exhibited several advantages and characteristics such as high degradation rate, good extent of degradation, applicability in a broad concentration range, and suitability for non-transparent solutions. Here, methyl orange (MO) was selected as a model compound because it is widely used in textile industries, but not easily biodegraded (see Fig. S1).

2. Materials and methods

2.1. Preparation of supported-TiO_2/AC

The granular activated carbon (Liaoning Medical Company, China) was made from coal and had ash content of 3–5%, particle size of 2–3 mm, surface area of 1300 m^2/g, and average pore diameter of 2–3 nm. AC was firstly ground and sieved out using 100 mesh sieve, and the powdery AC was obtained. As pretreatment, 10.0 g AC powder was weighted and added into 100 mL deionized water, and then boiled at 100 °C for 30 min. After the suspension was cooled to room temperature, the AC powder was filtered out, dried at 105 °C for 6.0 h and stored in a desiccator for use. For the preparation of TiO_2/AC, nano-TiO_2 powder (anatase, Harbin Chemistry Reagent Company, China) and AC powder in a certain mass ratio (0–16% TiO_2) were added into 100 mL deionized water and boiled at 100 °C for 30 min. Then the suspension was cooled to room temperature and the mixed powder was filtered out and calcined in a muffle furnace (SX2-4-10, Great Wall Furnace Company, China) at temperature rise rate of 10 °C/min and then maintained at constant temperature at 300 °C for 60 min. After fully grinding, the supported-TiO_2/AC was obtained.

2.2. Characterization of supported-TiO_2/AC

An X-ray diffraction (XRD, RINT 2500, XRD-RigakuU Corporation, Japan) analysis was performed using Ni-filtered Cu Kα radiation in the range of 2θ from 10° to 70° to study the crystal structure and crystallinity of the supported-TiO_2 nanoparticles on the surface of AC. The supported-TiO_2/AC particle morphology was characterized by a scanning electron microscope (SEM, JSM-6301F, LEO Corporation, England) at an accelerating voltage of 20 kV. Fourier transform infrared (FT-IR) spectra analysis was also carried out using FT-IR spectrometer (Nicolet Avatar 330, Nicolet Company, USA) to investigate the presence of the supported-TiO_2 on AC.

2.3. Experiment of TiO_2/AC/MW degradation

A 25 mL MO solution (50 mg/L) with natural pH close to 6.0 and 20.0 mg supported-TiO_2/AC powder (0.8 g/L) were added into a self-made glass reactor with a condenser. The system was installed in a controllable MW oven (WD750B, Guangdong Galanz Company, China) (see Fig. S2). The MW (750 W, 2450 MHz) was utilized to irradiate this suspension and the UV–vis spectra of MO were obtained using a UV–vis spectrophotometer (Cary 50, Varian Company, USA). In order to compare the degradation effects, control experiments of the MO solution treated by AC only or MW only were also conducted. The maximum absorbance (at 466 nm) of 0–60 mg/L MO solutions approximately abides the Lambert–Beer's law. The formula (% degradation = $[(C_0 - C)/C_0] \times 100$) was used to determine the % degradation of MO, where C_0 and C are the initial and instant (at reaction time t) concentrations of MO solution, respectively. Also, the effects of the mass ratio (0–10%) of TiO_2 in the catalyst mixture, MW irradiation time (0–5.0 min), initial MO concentration (10–90 mg/L), TiO_2/AC dose (0–2.0 g/L), and initial pH (2.0–10.0) on the degradation kinetics were investigated. Duplicate experiments were performed and the error was less than 2%. All the conditions were kept throughout the experiments, if not mentioned otherwise. All other reagents were of analytical grade and used as received. MilliQ-grade water (18.2 MΩ cm) was used throughout in this work.

MO samples were analyzed by high performance liquid chromatography (HPLC, Pro-210, Varian Company, USA) equipped with a UV detector set at 254 nm under isocratic conditions: 80% (v/v) of methanol in Milli-Q water with a flow rate of 1.0 mL/min. The column employed was a C18 reverse phase column (4.6 mm × 250 mm i.d.) with an injection volume of 20 μL. Also, the total organic carbon (TOC) of the samples was determined using a TOC analyzer (Elementar Analysensysteme, GmbH Company, Germany) with an IR detector. Oxygen carrier gas was kept at 0.95–1.00 bar. The flow rate was 200 mL/min and the injection volume was 10 μL. To determine the amount of nitrite/nitrate and sulfite/sulfate in the treated samples of MO, a Dionex ICS-90 Ion Chromatography (IC, Dionex Company, USA) with a conductivity detector was utilized. 9.0 mmol/L $NaCO_3$ was used as the eluent phase. An AS9-HC column (4.0 mm × 250 mm i.d.) was the most suitable for this analysis. The flow rate was 1.0 mL/min and the injection volume was 10 μL.

2.4. Determination of hydroxyl radical (•OH) in TiO_2/AC/MW system

A 25.00 mL 1,5-diphenyl carbazide (DPCI) aqueous solution and 100 mg supported-TiO_2/AC powder were added into a 250 mL conical flask. Another two shares with 100 mg AC alone or TiO_2 alone instead of the supported-TiO_2/AC were also used for comparison.

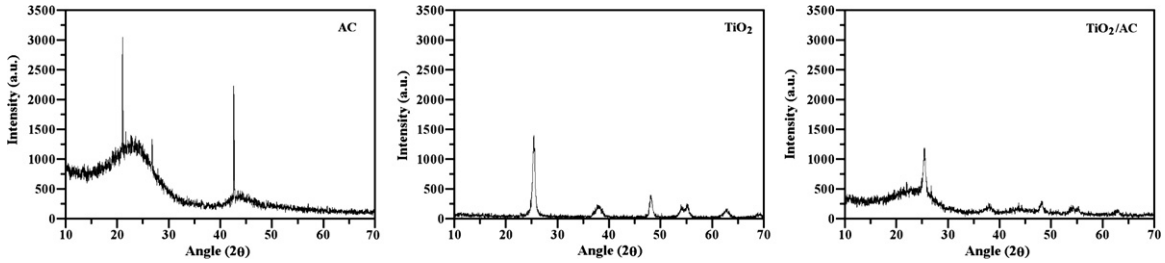

Fig. 1. XRD patterns of TiO_2/AC, TiO_2 alone and AC alone.

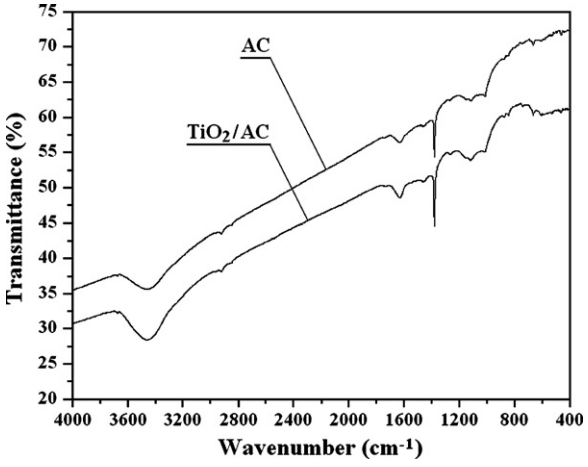

Fig. 2. FT-IR spectra of TiO_2/AC and AC alone.

Then, the MW was utilized to irradiate these suspensions within 2.0 min, respectively, using a controllable MW oven operating at 2450 MHz and 750 W. After the suspension was cooled to room temperature, a 10.0 mL solution was taken from each share solution and extracted with 10 mL mixed solvent of benzene and carbon tetrachloride (volume ratio = 1:1). Afterwards, the UV–vis spectra of the extracted solutions from water phase were measured at 563 nm that was the maximum absorption wavelength of 1,5-diphenyl carbazone (DPCO) [24].

3. Results and discussion

3.1. XRD, FT-IR and SEM of TiO_2/AC

Fig. 1 illustrates the XRD patterns of TiO_2/AC, TiO_2 and AC. The characteristic diffraction peaks at $2\theta = 25.4^\circ$, 38.0°, 48.0°, 54.7° and 63.1° were all designated to anatase crystal phase TiO_2 without any indication of other crystalline phases of TiO_2, such as rutile, under the analyzed conditions. Also, the main peaks attributed to AC could be found. The average crystallite sizes of TiO_2 in TiO_2/AC and TiO_2 alone particles are about 10.88 nm and 16.11 nm, respectively, according to the Scherrer equation: $D = K\lambda/(\beta \times \cos\theta)$ (where K is the constant equal to 0.89, λ is the X-ray wavelength equal to 0.154 nm, β is the full width at half maximum and θ is the half diffraction angle ($\theta = 12.7^\circ$)) [25]. It indicates a clear broader peak belonging to the 1 0 1 plane for the TiO_2 [26]. These results indicate that the anatase TiO_2 particles were well supported on the surface of AC powder.

As shown in Fig. 2, AC mainly shows one absorption peak and three absorption bands in the wavelength range from 4000 to 400 cm^{-1}. The two bands around 3410 and 1600 cm^{-1} are assigned to the stretch and bend vibrations of O—H, respectively, while the peak at 1400 cm^{-1} and the third band around 1060 cm^{-1} belong to the skeleton vibration [27]. However, comparing with the peaks of only AC, TiO_2/AC shows a different absorption band at around 600 cm^{-1}. It is assigned to the stretch vibration of Ti—O bond. Thus, TiO_2 particles are proved to be well-distributed on the surface of AC powder.

The SEM technique was used to verify the morphology and chemical composition of the TiO_2/AC powder. The SEM image of the TiO_2/AC in Fig. 3(a) shows the bulk form of the TiO_2/AC with a size of approximately 1.0–1.5 μm. Furthermore, as shown in Fig. 3(b), the morphology of TiO_2/AC exhibited a less condensed phase, distinct pore structure, and small TiO_2 nanoparticles with a size of approximately 50–150 nm uniformly distributed on the surface of AC. The supported-TiO_2 had not obvious influence on the morphology of the AC [16,28].

3.2. UV–vis spectra of MO solutions during TiO_2/AC/MW treatment

In order to compare the degradation effect of MO at different conditions, experiments with 50 mg/L MO solution at a

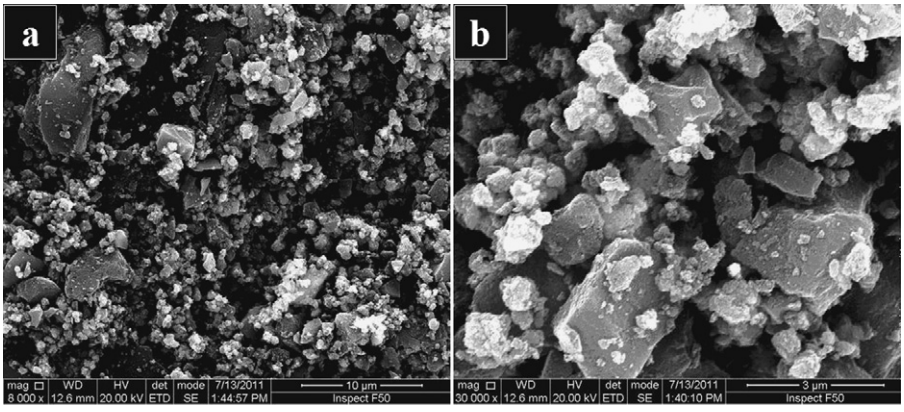

Fig. 3. SEM images of TiO_2/AC powder. (a) 10 μm and (b) 3 μm.

Table 1
C/C_0 of various absorption peaks of MO from UV–vis spectra. (50 mg/L MO, 750 W, 2450 MHz, 3.0 min MW, 0.8 g/L catalyst and pH = 6.0).

C/C_0	Systems				
	MW alone	TiO_2/AC	AC alone	AC/MW	TiO_2/AC/MW
Peak *A* (466 nm)	0.985	0.609	0.582	0.213	0.116
Peak *B* (270 nm)	0.993	0.648	0.629	0.265	0.189

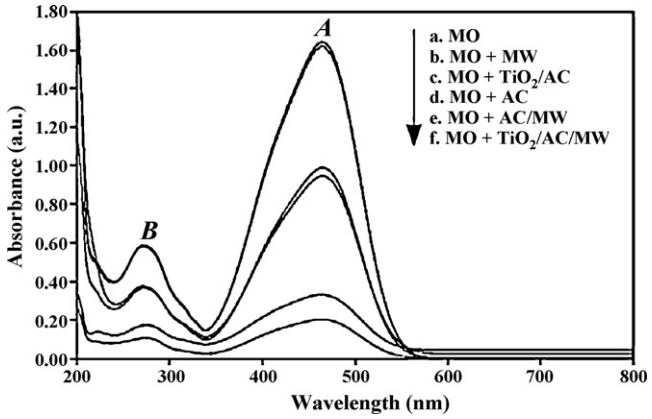

Fig. 4. UV–vis spectra of MO solutions during degradation. (50 mg/L MO, 750 W, 2450 MHz, 3.0 min MW, 0.8 g/L catalyst and pH = 6.0).

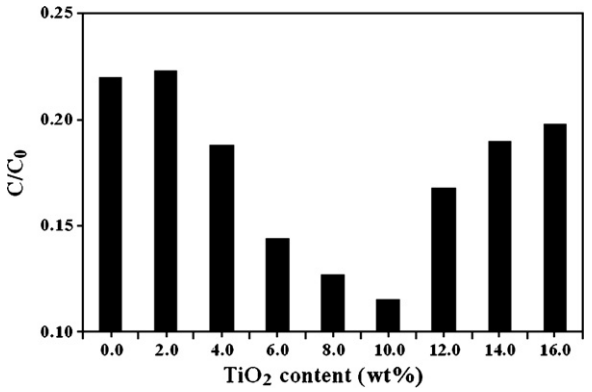

Fig. 5. Influence of TiO_2 content on TiO_2/AC/MW degradation. (50 mg/L MO, 750 W, 2450 MHz, 3.0 min MW, 0.8 g/L catalyst and pH = 6.0).

certain time were performed. MO solution mainly displays two absorption peaks located at 270 and 466 nm which belong to the benzene ring and —N=N— bond, respectively (see Fig. 4). The absorption peak declines a little bit for MW alone system without any catalyst, which indicates that MW alone has slow degradation kinetics. In addition, 39.1% and 41.8% adsorption of MO was observed in the TiO_2/AC and AC alone systems, respectively. Moreover, when the AC/MW or TiO_2/AC/MW system was used, the absorption peaks decreases significantly. It implies that enhanced degradation of MO occurs in the presence of AC or TiO_2/AC under MW irradiation [20]. It is because AC can strongly absorb MW energy and "hot spots" can form on its surface. The organic pollutant, like MO, around the "hot spots" can be readily oxidized or nearly burned. Particularly, the TiO_2/AC/MW system achieved 88.4% degradation within 3.0 min of MW irradiation. It may be inferred that the supported-TiO_2 particles that can achieve the heat energy of "hot spots" on AC under MW irradiation. Then, some electrons may transfer through thermal excitation and the electron–hole pairs may form on the surface of TiO_2, which could help the oxidation of the MO [23]. The following systems are listed in order of decreasing degradation rates of MO: supported-TiO_2/AC/MW > AC/MW > AC alone > supported-TiO_2/AC > MW alone. Otherwise, the absorption peaks at 466 (*A*) and 270 nm (*B*) fall almost synchronously, which indicates that not only the azo bond but also the benzyl ring in MO molecule can be destroyed mostly in the TiO_2/AC/MW system (see Table 1).

3.3. Influence of TiO_2 content on TiO_2/AC/MW degradation

Fig. 5 shows that the extent of degradation increases with increasing TiO_2 added wt.% content from 0 to 10.0%, and then drops to some extent at ratio 10.0–16.0% TiO_2. This is because at the lower proportion, the TiO_2 can effectively obtain heat energy from the "hot spots" on the surface of AC and be excited to form electron–hole pairs, which would favor enhanced oxidation of MO. But when much TiO_2 is supported, the particles may cover the activated sites of AC and disturb MW transmission, which can prevent MO from approaching the activated sites. The optimal added proportion was fixed at 10 wt.% throughout the remaining of the study.

3.4. Influence of MW irradiation time on degradation in the TiO_2/AC/MW process

Fig. 6(a) shows that the decrease extent increases from 39.1% to 96.1% with increasing MW irradiation time (0.0–5.0 min) in TiO_2/AC/MW system, while for AC/MW system, it increased from 41.8% to 88.3% under the same conditions. Also, the adsorption of TiO_2/AC (39.1%) was smaller than that of AC alone (41.8%). These

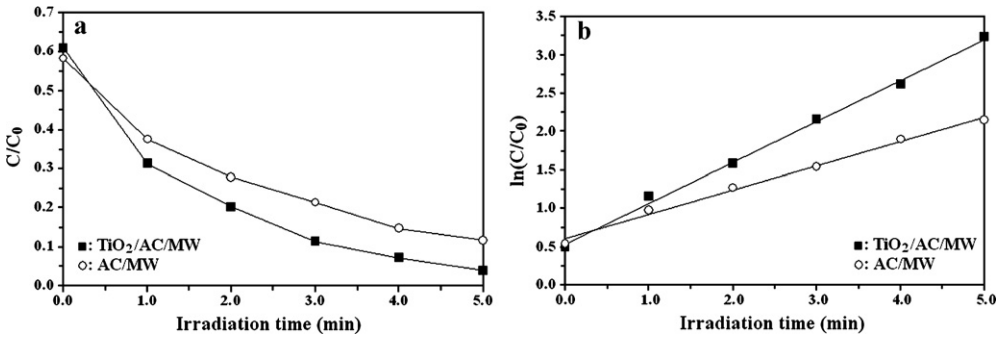

Fig. 6. Influence of MW irradiation time (a) and kinetics (b) on TiO_2/AC/MW degradation. (50 mg/L MO, 750 W, 2450 MHz, 0.8 g/L catalyst and pH = 6.0).

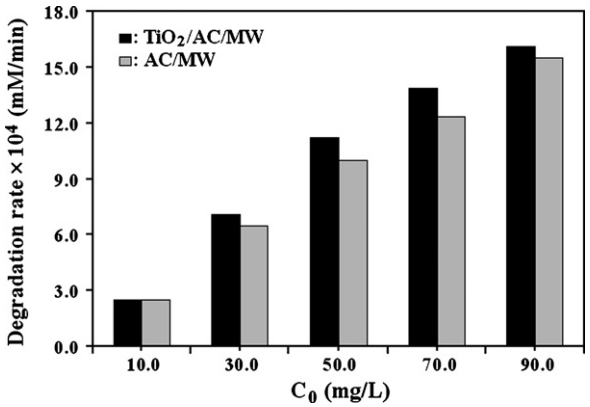

Fig. 7. Influence of C_0 on TiO_2/AC/MW degradation. (0.8 g/L catalyst, 750 W, 2450 MHz, 3.0 min MW, pH = 6.0).

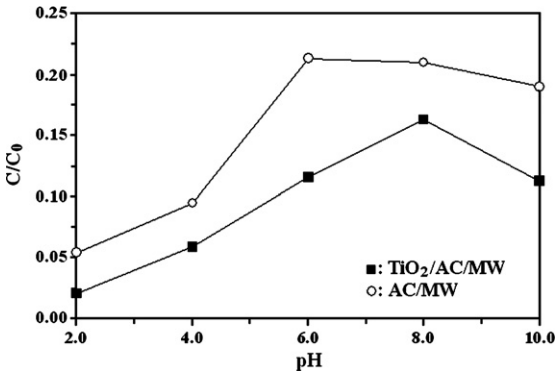

Fig. 8. Influence of initial pH on TiO_2/AC/MW degradation. (50 mg/L MO, 0.8 g/L catalyst, 750 W, 2450 MHz and 3.0 min MW).

results indicate that the catalytic activity of TiO_2/AC is higher than that of AC alone. This can be attributed to the heat energy obtained by the TiO_2 particles.

In order to determine the kinetics of degradation reactions, the data of $-\ln(C/C_0)$ for first-order reaction and $1/C_t$ for second-order reaction versus irradiation time (t) were all calculated and checked for the two cases. Firstly, the adsorption results in the straight lines do not pass through the origin in Fig. 6(b). Secondly, Fig. 6(b) shows a good linear relationship between $-\ln(C/C_0)$ and t for low concentration (50 mg/L) of organic pollutants. It demonstrates that the degradation rate appears to fit the pseudo-first order kinetics for concentrations between 10 and 50 (or 70) mg/L since the initial rate increases proportionately with C_0 (see Fig. 7). The rate constants (k) are 0.534 and 0.316 min^{-1} for TiO_2/AC/MW and AC/MW systems, respectively. Apparently, the more effective degradation is achieved for TiO_2/AC/MW system within the range of this concentration (10–50 mg/L). But the data at 70–90 mg/L are not fitted well using the pseudo first-order kinetic model since under these conditions the dye is in excess and the reactions are limited by the concentration of •OH radicals.

Furthermore, the results show that the extent of mineralization calculated from TOC values are 63.0% and 88.1% within 1.0 and 5.0 min MW irradiation, respectively, for the TiO_2/AC/MW system. This is consistent with the results based on UV–vis spectra for the degradation of MO. They both indicate that the MO can be almost completely mineralized in the TiO_2/AC/MW treatment process.

3.5. IC and HPLC of MO solution during TiO_2/AC/MW degradation

Since MO molecule contains nitrogen and sulfur atoms, the NO_3^- and SO_4^{2-} ions are expected to be among the degradation byproducts. An obvious peak belonging to SO_4^{2-} appears at retention time of 17.4 min and another NO_3^- peak does at 12.3 min retention time (see Fig. S3(a)). It indicates that a number of SO_4^{2-} and a small quantity of NO_3^- ions are produced during MO degradation in the two systems. The area of these peaks became larger and larger with increasing irradiation time, which means that the C—S, C—N and N=N bonds of MO have been rapidly broken even within a short irradiation time.

Quantification of MO using HPLC was determined considering the absorbance at 254 nm (see Fig. S3(b)). The maximum absorption peak appeared at about 1.45 min retention time. The area of this peak became smaller and smaller with increasing irradiation time, which meant that the benzene ring of MO molecule was destroyed. Also, no intermediates were detected using the analytical methods employed in this work, since most probably the intermediates that were formed were also degraded rapidly and completely. Therefore, both IC and HPLC analyses verified that all MO molecules could be rapidly degraded and almost mineralized to simple inorganic ions within short treatment time using the TiO_2/AC/MW technology.

3.6. Influence of initial concentration (C_0) on TiO_2/AC/MW degradation

Results on the comparison of degradation rates of MO after 3.0 min of reaction time are shown in Fig. 7 for the two systems. For the MO solution at 10–70 mg/L in TiO_2/AC/MW system, a degradation rate of 2.5×10^{-4} to 13.9×10^{-4} mmol/min was observed, while this represents a MO complete degradation (below detection limit) to 77.8% degradation, respectively, within 3.0 min. Also, the degradation rate increased with increasing C_0 as expected when other conditions are kept constant (10–70 mg/L). But this did not happen at higher concentrations (70–90 mg/L) because the solutions contain a larger number of organics molecules, limited amount of catalysts, and the reactions are limited by the concentration of •OH radicals. Hence, the extent of degradation for any specific C_0 for the TiO_2/AC/MW system was again found to be always higher than that for AC/MW system, which resulted from the higher number of active sites on the surfaces of TiO_2/AC compared to AC alone under MW irradiation.

3.7. Influence of initial pH on TiO_2/AC/MW degradation

The number of available adsorption sites on the catalyst is affected by changes of solution pH. Also, pH changes can also alter the overall charge of the contaminants and the catalyst, and consequently the adsorption rate on the active sites of the catalyst [29]. Fig. 8 shows the extent of degradation first decreases and then increases. At pH = 8.0 (or pH = 6.0), the extent of degradation becomes the lowest for TiO_2/AC (or AC alone) system which reveals this case is much susceptible to pH.

The isoelectric points (pH_{IEP}) of AC and TiO_2 particles were determined to be about 6.0 [30]. When the pH value is lower than pH_{IEP} of AC and TiO_2, TiO_2 and AC particles possess positive charge while a negative charge is expected at higher pH ($pH > pH_{IEP}$). MO with negative charge after ionization is strongly attracted to the surface of the catalyst which can enhance degradation. Above pH_{IEP}, the surface of TiO_2/AC is negatively charged. Thus, electrostatic repulsion may occur between MO and the catalysts, resulting in the decrease of the degradation efficiency. In addition, alkaline pH conditions can help in the production of •OH radicals, which assists in the degradation through •OH radical oxidation mechanism. All of these can promote the degradation of MO and the reaction intermediates. Consequently, TiO_2/AC exhibits higher catalytic activity in acidic and alkaline solutions. Considering kinetics, the TiO_2/AC/MW catalytic system appears to be more preferable in the study.

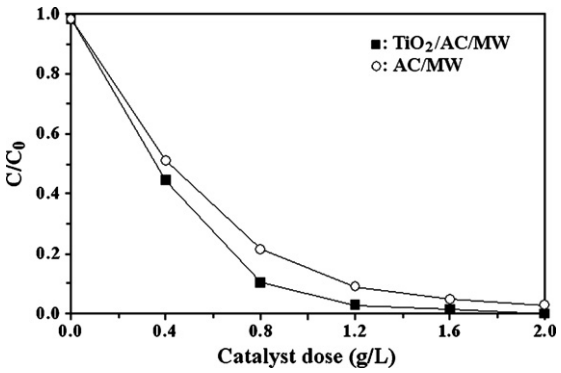

Fig. 9. Influence of catalyst dose on TiO_2/AC/MW degradation. (50 mg/L MO, 750 W, 2450 MHz, 3.0 min MW and pH = 6.0).

3.8. Influence of catalyst dose on TiO_2/AC/MW degradation

Considering the extent of degradation and economic removal of dye pollutants, it is important to determine the optimum dose of catalyst. Fig. 9 shows that in the low dose range (below 0.8 g/L) the degradation extent increases rapidly with increasing catalyst dose, while at high dose (above 0.8 g/L), it does slowly. The degradation reached 89.6% using 0.8 g/L TiO_2/AC, while it was 78.7% for 1.2 g/L AC alone. The results also show that the extent of degradation increases only slightly at catalyst dose higher than 1.2 g/L. Anyway, the degradation extent for TiO_2/AC/MW system was higher at all catalyst doses reaching complete degradation at a catalyst dose of 2.0 g/L. Here, 0.80 g/L was adopted throughout the remaining experiments.

3.9. Generation of •OH radicals in TiO_2/AC/MW system

The determination of •OH radicals was carried out through the oxidation of 1,5-diphenyl carbazide (DPCI) to 1,5-diphenyl carbazone (DPCO) [31]. The DPCO can be extracted by the mixed solvent of benzene and carbon tetrachloride and this extract liquor displays an obvious absorption peak located at 563 nm that belongs to the —N=N— bond of DPCO (see Fig. 10) [24]. In addition, the absorbance decreased after the addition of vitamin C (VC) which acts as the •OH radical scavenger agent [32]. By comparison, the absorption peak at 563 nm in the TiO_2/AC system decreased the most when VC was added, which suggests that the MW can directly excite the semiconductor TiO_2 to carry out oxidation reaction with high efficiency. Therefore, it has been shown that nano-TiO_2 can be

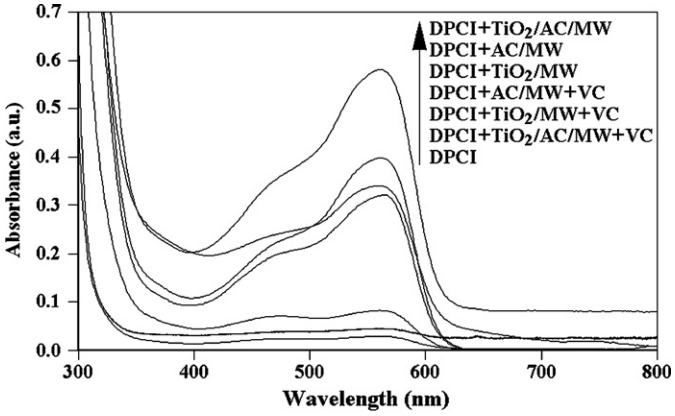

Fig. 10. UV–vis spectra of DPCO extract liquors in the presence of TiO_2/AC or AC alone under MW irradiation. ([DPCI] = 2.5×10^{-3} mol/L, [VC] = 0.1 mol/L, TiO_2/AC (or AC alone) = 0.4 g/L and 2.0 min MW).

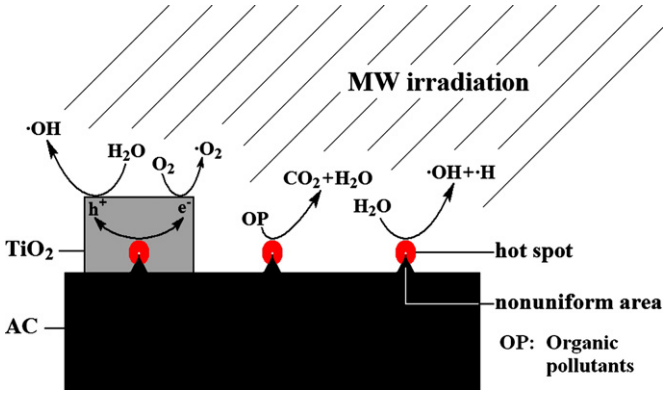

Fig. 11. Possible mechanism on catalytic reaction of TiO_2/AC/MW degradation.

used to help produce •OH for enhancing AC/MW degradation rates of recalcitrant organic contaminants and reaction intermediates formed.

3.10. Possible mechanism on catalytic reaction of TiO_2/AC/MW degradation

Organic pollutants can be degraded in AC/MW system, a process referred to as MW-induced oxidation [20,27]. AC particles can strongly absorb MW energy and then generate many "hot spots" on their surface [33]. The organic pollutants around the "hot spots" can be decomposed in the presence of oxygen (O_2) dissolved in water. It is considered to be a process being similar to combustion oxidation. In the present study, nano-TiO_2 particles were supported on the surface of AC further assisting AC/MW degradation (see Fig. 11). The temperature of "hot spot" on the surface of AC under MW irradiation in water medium can achieve 1200 °C or more. It results in significant increase in the number of activated sites and brings many holes to produce hydroxyl radical (•OH) on the surface of semiconductor catalyst in the solution. The supported-TiO_2 is able to absorb the heat energy of "hot spots" and can be excited to generate the electron–hole pairs that would react with O_2 and H_2O to form •OH and superoxide radical anion ($O_2^{\bullet -}$). Finally, the $O_2^{\bullet -}$ can also yield •OH through a series of chemical reactions [13]. Thus, the degradation rates can be increased. In brief, supported-TiO_2/AC can be adopted as a catalyst to help produce more activated sites on the surface of AC and much •OH radicals in the solution under MW irradiation, which is expected to increase the rates of degradation of recalcitrant organic contaminants and reaction intermediates formed.

4. Conclusions

The combination of supported nano-TiO_2 on the surface of AC and MW (TiO_2/AC/MW) was applied to enhance the MW-induced degradation of azo dye in the aqueous solution. Methyl orange (MO) was selected as a model contaminant. It has been found the supported-TiO_2 on the surface of AC can be excited resulting in the production of •OH in the aqueous solution under MW irradiation, which significantly enhanced the performance of AC/MW process for the degradation of MO. Also, the TiO_2/AC system displayed higher catalytic activity than AC alone under MW irradiation.

Under the conditions applied of 50 mg/L and 25 mL MO solution, 2.0 g/L catalyst dose, 750 W, 2450 MHz MW, and solution pH = 6.0, complete degradation was obtained using the TiO_2/AC/MW system within 1.5 min MW irradiation. Overall, the integrated TiO_2/AC/MW advanced oxidation technology exhibited several advantages, including high degradation rate, short irradiation time, no residual intermediates, and no secondary pollution. Therefore,

it shows to be a promising technology for the destruction of organic contaminants in azo dye treatment applications.

Acknowledgments

The authors greatly acknowledge The Science Research Plan Project (L2010156) and Environmental Science Key Discipline Construction Project of Liaoning Province Education Department of China, "211" Project of Liaoning University, The Key Laboratory of Water Environment Biomonitoring and Ecological Security of Liaoning Province and Startup Foundation for Doctors of Liaoning University of China for financial support. The authors also thank our colleagues and other students assisting in this work.

Appendix A. Supplementary data

Supplementary data associated with this article can be found, in the online version, at doi:10.1016/j.jhazmat.2012.01.021.

References

[1] O.D. Olukanni, A.A. Osuntoki, G.O. Gbenle, Textile effluent biodegradation potentials of textile effluent-adapted and non-adapted bacteria, Afr. J. Biotechnol. 5 (2006) 1980–1984.
[2] M.A. Kamboh, I.B. Solangi, S.T.H. Sherazi, S. Memon, A highly efficient calix[4] arene based resin for the removal of azo dyes, Desalination 268 (2011) 83–89.
[3] S. Song, H.P. Ying, Z.Q. He, J.M. Chen, Mechanism of decolorization and degradation of CI direct red 23 by ozonation combined with sonolysis, Chemosphere 66 (2007) 1782–1789.
[4] Z.J. Hu, Y. Xiao, D.H. Zhao, Y.L. Shen, H.W. Gao, Preparation of dye waste–barium sulfate hybrid adsorbent and application in organic wastewater treatment, J. Hazard. Mater. 175 (2010) 179–186.
[5] Y.Y. Qu, S.N. Shi, F. Ma, B. Yan, Decolorization of reactive dark blue K-R by the synergism of fungus and bacterium using response surface methodology, Bioresour. Technol. 101 (2010) 8016–8023.
[6] K.L.S. Ahmed, S. Sajjad, B.Z. Tian, F. Chen, J.L. Zhang, Comparative studies of operational parameters of degradation of azo dyes in visible light by highly efficient WO_x/TiO_2 photocatalyst, J. Hazard. Mater. 177 (2010) 781–791.
[7] S.A. Ong, K. Uchiyama, D. Inadama, K. Yamagiwa, Simultaneous removal of color, organic compounds and nutrients in azo dye-containing wastewater using up-flow constructed wetland, J. Hazard. Mater. 165 (2009) 696–703.
[8] F. Han, V. Subba, R. Kambala, M. Srinivasan, D. Rajarathnam, R. Naidu, Tailored titanium dioxide photocatalysts for the degradation of organic dyes in wastewater treatment: a review, Appl. Catal. A: Gen. 359 (2009) 25–40.
[9] W.J. Lau, A.F. Ismail, Polymeric nanofiltration membranes for textile dye wastewater treatment: preparation performance evaluation, transport modelling, and fouling control—a review, Desalination 245 (2009) 321–348.
[10] F. Harrelkas, A. Azizi, A. Yaacoubi, A. Benhammou, M.N. Pons, Treatment of textile dye effluents using coagulation–flocculation coupled with membrane processes or adsorption on powdered activated carbon, Desalination 235 (2009) 330–339.
[11] Y. Ao, J.J. Xu, D.G. Fu, C.W. Yuan, Photocatalytic degradation of X-3B by titania-coated magnetic activated carbon under UV and visible irradiation, J. Alloys Compd. 471 (2009) 33–38.
[12] J.Q. Gao, X.Y. Luan, J. Wang, B.X. Wang, K. Li, Y. Li, P.L. Kang, G.X. Han, Preparation of Er^{3+}:$YAlO_3$/Fe-doped TiO_2–ZnO and its application in photocatalytic degradation of dyes under solar light irradiation, Desalination 268 (2011) 68–75.
[13] J. Wang, G. Zhang, Z.H. Zhang, X.D. Zhang, G. Zhao, F.Y. Wen, Z.J. Pan, Y. Li, P. Zhang, P.L. Kang, Investigation on photocatalytic degradation of ethyl violet dyestuff using visible light in the presence of ordinary rutile TiO_2 catalyst doped with upconversion luminescence agent, Water Res. 40 (2006) 2143–2150.
[14] S.S. Horikoshi, M.T. Kajitani, S.M. Sato, N. Serpone, A novel environmental risk-free microwave discharge electrodeless lamp (MDEL) in advanced oxidation processes: degradation of the 2,4-D herbicide, J. Photochem. Photobiol. A: Chem. 189 (2007) 355–363.
[15] X.T. Liu, X. Quan, L.L. Bo, S. Chen, Y.Z. Zhao, Simultaneous pentachlorophenol decomposition and granular activated carbon regeneration assisted by microwave irradiation, Carbon 42 (2004) 415–422.
[16] Z. He, S.G. Yang, Y.M. Ju, C. Sun, Microwave photocatalytic degradation of Rhodamine B using TiO_2 supported on activated carbon: mechanism implication, J. Environ. Sci. 21 (2009) 268–272.
[17] Y.Z. Liu, S.G. Yang, J. Hong, C. Sun, Low-temperature preparation and microwave photocatalytic activity study of TiO_2-mounted activated carbon, J. Hazard. Mater. 142 (2007) 208–215.
[18] X.J. Wang, Y.F. Liu, Z.H. Hu, Y.J. Chen, W. Liu, G.H. Zhao, Degradation of methyl orange by composite photocatalysts nano-TiO_2 immobilized on activated carbons of different porosities, J. Hazard. Mater. 169 (2009) 1061–1067.
[19] S.X. Liu, X.Y. Chen, X. Chen, A TiO_2/AC composite photocatalyst with high activity and easy separation prepared by a hydrothermal method, J. Hazard. Mater. 143 (2007) 257–263.
[20] Z.H. Zhang, Y.B. Shan, J. Wang, H.J. Ling, S.L. Zang, W. Gao, Z. Zhao, H.C. Zhang, Investigation on the rapid degradation of Congo red catalyzed by activated carbon powder under microwave irradiation, J. Hazard. Mater. 147 (2007) 325–333.
[21] Z.H. Zhang, Y.Q. Deng, M.L. Shen, W.M. Han, Z.L. Chen, D.P. Xu, X.T. Ji, Investigation on the rapid degradation of sodium dodecyl benzene sulfonate (SDBS) under microwave irradiation in the presence of modified activated carbon powder with ferrous sulfate, Desalination 249 (2009) 1022–1029.
[22] Z. Zhang, D. Xu, M. Shen, D. Wu, Z. Chen, X. Ji, F. Li, Y. Xu, Degradation of surfactant wastewater under microwave irradiation in the presence of activated carbon assisted with nano-sized TiO_2 or nano-sized ZnO, Water Sci. Technol. 63 (2011) 424–431.
[23] J. Wang, W. Sun, Z.H. Zhang, Z. Jiang, X.F. Wang, R. Xu, R.H. Li, X.D. Zhang, Preparation of Fe-doped mixed crystal TiO_2 catalyst and investigation of its sonocatalytic activity during degradation of azo fuchsine under ultrasonic irradiation, J. Colloid Interface Sci. 320 (2008) 202–209.
[24] Y.W. Guo, C.P. Cheng, J. Wang, Z.Q. Wang, X.D. Jin, K. Li, Detection of reactive oxygen species (ROS) generated by TiO_2(R), TiO_2(R/A) and TiO_2(A) under ultrasonic and solar light irradiation and application in degradation of organic dyes, J. Hazard. Mater. 172 (2011) 786–793.
[25] H. Slimena, A. Houas, J.P. Nogier, Elaboration of stable anatase TiO_2 through activated carbon addition with high photocatalytic activity under visible light, J. Photochem. Photobiol. A: Chem. 221 (2011) 13–21.
[26] M. Pelaez, A.A. De la Cruz, E. Stathatos, P. Falaras, D.D. Dionysiou, Visible light-activated N-F-codoped TiO_2 nanoparticles for the photocatalytic degradation of microcystin-LR in water, Catal. Today 144 (2009) 19–25.
[27] X.T. Liu, G. Yu, W.Y. Han, Granular activated carbon adsorption and microwave regeneration for the treatment of 2,4,5-trichlorobiphenyl in simulated soil-washing solution, J. Hazard. Mater. 147 (2007) 746–751.
[28] B.F. Gao, P.S. Yap, T.M. Lim, T.T. Lim, Adsorption–photocatalytic degradation of acid red 88 by supported TiO_2: effect of activated carbon support and aqueous anions, J. Chem. Eng. 171 (2011) 1098–1107.
[29] M.G. Antoniou, D.D. Dionysiou, Application of immobilized titanium dioxide photocatalysts for the degradation of creatinine and phenol, model organic contaminants found in NASA's spacecrafts wastewater streams, Catal. Today 124 (2007) 215–223.
[30] S.J. Park, S.S. Chin, Y. Jia, A.G. Fane, Regeneration of PAC saturated by bisphenol A in PAC/TiO_2 combined photocatalysis system, Desalination 250 (2010) 908–914.
[31] J. Wang, Y.W. Guo, B. Liu, X.D. Jin, L.J. Liu, R. Xu, Y.M. Kong, B.X. Wang, Detection and analysis of reactive oxygen species (ROS) generated by nano-sized TiO_2 powder under ultrasonic irradiation and application in sonocatalytic degradation of organic dyes, Ultrason. Sonochem. 18 (2011) 177–183.
[32] J. Wang, Y.W. Guo, J.Q. Gao, X.D. Jin, Z.Q. Wang, B.X. Wang, K. Li, Y. Li, Detection and comparison of reactive oxygen species (ROS) generated by chlorophyllin metal (Fe, Mg and Cu) complexes under ultrasonic and visible-light irradiation, Ultrason. Sonochem. 18 (2011) 1028–1034.
[33] X. Quan, Y.B. Zhang, S. Chen, Y.Z. Zhao, H.M. Zhao, F.L. Yang, Generation of hydroxyl radical in aqueous solution by microwave energy using activated carbon as catalyst and its potential in removal of persistent organic substances, J. Mol. Catal. A: Chem. 263 (2007) 216–222.